International Journal of Bifurcation and Chaos

Controlling chaos of hybrid systems by variable threshold values

Daisuke Ito
Advanced Tech. and Science, System Innovation Engineering, University of Tokushima,
2-1 Minami-Jousanjima, Tokushima, 770-8504, Japan
d-ito@is.tokushima-u.ac.jp

Tetsushi Ueta
Center for Admin. Info. Tech., University of Tokushima,
2-1 Minami-Jousanjima, Tokushima, 770-8504, Japan
ueta@tokushima-u.ac.jp

Takuji Kousaka
Department of Mechanical and Energy Systems Engineering, Oita University,
700 Dannoharu, Oita, 870-1192, Japan
takuji@oita-u.ac.jp

Jun'ichi Imura
Department of Mechanical and Environmental Informatics, Tokyo Institute of Technology,
2-12-1 Ookayama Meguro-ku, Tokyo, 152-8552, Japan
imura@mei.titech.ac.jp

Kazuyuki Aihara
Institute of Industrial Science, University of Tokyo,
4-6-1 Komaba Meguro-ku, Tokyo, 152-8505, Japan
aihara@sat.t.u-tokyo.ac.jp

Received (to be inserted by publisher)

We try to stabilize unstable periodic orbits embedded in a given chaotic hybrid dynamical system by a perturbation of a threshold value. In conventional chaos control methods, a control input is designed by state-feedback, which is proportional to the difference between the target orbit and the current state, and it is applied into a specific system parameter or the state as a small perturbation. During a transition state, the control system consumes a certain control energy given by integration of such perturbations. In our method, we change the threshold value dynamically to control the chaotic orbit. Unlike the OGY method and the delayed feedback control, no actual control input is added into the system. The state-feedback is utilized only to determine the dynamic threshold value, thus the orbit starting from the current threshold value reaches the next controlled threshold value without any control energy. We obtain the variation of the threshold value from the composite Poincaré map, and the controller is designed by the linear feedback theory with this variation. We demonstrate this method in simple hybrid chaotic systems and show its control performances with evaluating basins of attraction.

Keywords: controlling chaos, hybrid system, switching threshold

1. Introduction

Chaotic phenomena are observed in various deterministic dynamical systems including nonlinear electric circuits. They are characterized by the sensitivity to small perturbations, and also by the their complex orbit structure. It has been mathematically confirmed that an infinitely number of unstable periodic orbits (UPOs) are embedded in a chaotic attractor [Auerbach *et al.*, 1987]. An epoch-making control method called the Ott-Grebogi-Yorke (OGY) method was developed in 1990 [Ott *et al.*, 1990]. The control scheme pushes the orbit near the stable manifold of the target UPO with very small parameter perturbations. If it fails, one can expect another chance in near future because of the recurrent property of the chaos, i.e., the uncontrol orbit will comes close to the target UPO again. Therefore, it is possible to stabilize the target UPO with reasonably small control input, which is related to the distance between the current state and the UPO. Other methods to control chaos exist, including delayed feedback control [Pyragas, 2006] and its extension [Perc & Marhl, 2004, 2006], external force control [Pyragas, 1992], occasional proportional feedback [Roy *et al.*, 1992], and so on [Starrett, 2003; Myneni *et al.*, 1999; Rajasekar & Lakshmanan, 1993; Zambrano & Sanjuán, 2009; Sabuco *et al.*, 2010]. The controlling chaos utilizing the pole assignment method has also been proposed [Romeiras *et al.*, 1992]. Further an open loop controlling method has been investigated [Rajasekar, 1993]. Thanks to the Poincaré mapping a UPO in a continuous-time system can be expressed as an unstable periodic point (UPP) in the corresponding discrete-time system [Ueta & Kawakami, 1995]. To stabilize UPPs, therefore, the feedback gain of the controller can be designed with assigned poles regarding the characteristic equation for the variational equation [Ueta & Kawakami, 1995; Kousaka *et al.*, 2002]. Extensions of the methods are applied to chaotic hybrid systems [Kousaka *et al.*, 2006]. In these conventional methods, the amplitude of the control input is basically proportional to the error between the current state of the orbit and the UPP. Since the recurrence property of chaotic dynamics guarantees that the orbit will come close to the UPP in future, the control input can be small at this opportunity. However, in the previous study, the control input is added to the state or parameters of the system. Thus the controller must change them, which may be difficult to be changed in some of systems; e.g., in electrical circuits, the controller has to change the capacitor voltage, registers, and so on.

While, hybrid systems has been intensively studied for a decade [Leine & Nijmeijer, 2004]. In those systems, a flow described by a differential equation is interrupted by the discrete events, and then an impulsive jumping or a switching of the governing differential equation happens. Thus the flow may changes non-smoothly, and it may cause bifurcations [Bernardo *et al.*, 2008]; e.g., in chaotic spiking oscillators [Inagaki & Saito, 2008], a state-dependent switching generates two different flows. The authors show that a bifurcation phenomena and a chaotic response are guaranteed theoretically. In general, the switching mechanism is not explicitly described in the differential equations, but it affects certainly behavior of the system [Ito *et al.*, 2010; Kousaka *et al.*, 1999]. In electric circuits, a variable threshold is realized by an analog switch (multiplexer); therefore, to choose the threshold value as a control input is reasonable.

For a specific hybrid system, the controlling chaos based on the linear control theory can be realized by applying the Poincaré section on the border [Kousaka *et al.*, 2006]. UPPs in the derived discrete-time system are controlled with the same framework of the conventional control method, i.e., the control input is added into a system parameter or the state as a small perturbation successively. As far as the authors know, a threshold value in the given hybrid system is not used as the control parameter because dynamical affection with perturbed threshold value has not been evaluated yet. In the previous study [Ito *et al.*, 2010] we clarified the derivatives and variational equations of the given hybrid systems about threshold values. Thereby we apply these results to controlling chaos; namely, we try to design theoretically a control scheme with variations of threshold values in this paper.

Our purpose is to stabilize a UPO embedded within a chaotic attractor in a hybrid systems by varying their threshold value. The control system compares the current state variable with the threshold value, and updates the threshold value instantly and slightly. The orbit starting from the current Poincaré section (the threshold value) does not receive any control until it reaches the next section. Although K. Murali, *et al.* [Murali & Sinha, 2003] have proposed a chaos controller by featuring the perturbation of attached threshold values, the objective system is not a hybrid system and the proposed controller stabilizes UPOs

by clipping the voltage of a system with a simple circuit. Parameter values of the controller are provided by trial and error. In our method, the control vector is computed systematically by applying the linear control theory. We demonstrate control results of a 1D switching chaotic system and a 2D chaotic neuron, and evaluate its control performances of the controller by specifying basins of attraction. Moreover, a laboratory experiment is given for the former system.

2. Controller with perturbation of the threshold

Let us consider the n-dimensional and m-tuple differential equations described by

$$\frac{d\boldsymbol{x}}{dt} = \boldsymbol{f}_i(\boldsymbol{x}),\ i = 0,\ 1,\ \ldots,\ m-1, \tag{1}$$

where $t \in \boldsymbol{R}$ is time, $\boldsymbol{x} \in \boldsymbol{R}^n$ is the state and $\boldsymbol{f}_i :\ \boldsymbol{R}^n \to \boldsymbol{R}^n$ is a C^∞ class function.

Suppose that Π_i is a transversal section to the orbit and put $\boldsymbol{x}_0 = \boldsymbol{x}(0) \in \Pi_0$, then the solution of Eq. (1) is given by

$$\boldsymbol{x}(t) = \boldsymbol{\varphi}(\boldsymbol{x}_0, t). \tag{2}$$

Now we provide Π_i with a threshold value as follows:

$$\Pi_i = \{\boldsymbol{x} \in \boldsymbol{R}^n |\ q_i(\boldsymbol{x},\ \theta_i) = 0\}, \tag{3}$$

where q_i is a differentiable scalar function, and θ_i is a unique parameter that defines the position of Π_i. Note that Π_i becomes also a local section, and θ_i is independent from the vector field in Eq. (1). When an orbit governed by $\boldsymbol{f}_i$ reaches the section Π_i, the governing function is changed to $\boldsymbol{f}_{i+1}$. If the orbit passing through several sections reaches Π_0 again, then m local maps are defined as follows:

$$\begin{aligned}
T_0 &: \Pi_0 \to \Pi_1, \\
&\quad \boldsymbol{x}_0 \mapsto \boldsymbol{x}_1 = \boldsymbol{\varphi}_0(\boldsymbol{x}_0,\ \tau_0), \\
T_1 &: \Pi_1 \to \Pi_2, \\
&\quad \boldsymbol{x}_1 \mapsto \boldsymbol{x}_2 = \boldsymbol{\varphi}_1(\boldsymbol{x}_1,\ \tau_1), \\
&\quad \vdots \\
T_{m-1} &: \Pi_{m-1} \to \Pi_0, \\
&\quad \boldsymbol{x}_{m-1} \mapsto \boldsymbol{x}_0 = \boldsymbol{\varphi}_{m-1}(\boldsymbol{x}_{m-1},\ \tau_{m-1}),
\end{aligned} \tag{4}$$

where τ_i is the passage time from Π_i to Π_{i+1}, and depends on the state $\boldsymbol{x}_i$ and the parameter θ_{i+1} of the local section Π_{i+1}. Assume that $\boldsymbol{y}(k) \in \Sigma \subset \boldsymbol{R}^{n-1}$ is a location on local coordinates, then there is the projection satisfying $\eta(\boldsymbol{x}(k)) = \boldsymbol{y}(k)$. Let the composite map of T_i, $i = 0,\ 1, \ldots, m-1$ be the solution starting in $\eta^{-1}(\boldsymbol{y}(0)) = \boldsymbol{x}(0) \in \Pi_0$. From Eq. (4), the Poincaré map T is given by the following composite map:

$$T(\boldsymbol{y}(k),\ \theta_0,\ \theta_1,\ \ldots,\ \theta_{m-1}) = \eta \circ T_{m-1} \circ \cdots \circ T_1 \circ T_0 \circ \eta^{-1}. \tag{5}$$

Thus

$$\boldsymbol{y}(k+1) = T(\boldsymbol{y}(k),\ \theta_0,\ \theta_1,\ \ldots,\ \theta_{m-1}). \tag{6}$$

When the orbit starting from $\boldsymbol{x}_0 \in \Pi_0$ returns $\boldsymbol{x}_0$ itself, this orbit forms a periodic orbit and it is defined as the fixed point by using the Poincaré map T as follows:

$$\boldsymbol{y}_0 = T(\boldsymbol{y}_0,\ \theta_0,\ \ldots,\ \theta_{m-1}). \tag{7}$$

The corresponding characteristic equation is given by

$$\chi(\mu) = \det\left(\frac{\partial T(\boldsymbol{y}_0)}{\partial \boldsymbol{y}_0} - \mu I\right) = 0. \tag{8}$$

To apply the pole assignment method, the derivatives of the Poincaré map are required to compute a control gain [Ott *et al.*, 1990]. The equations in (4) are, in fact, differentiable with respect to the state, thus each derivatives is given as follows:

$$\frac{\partial T_i}{\partial \boldsymbol{x}_i} = \left[I - \frac{1}{\dfrac{\partial q_{i+1}}{\partial \boldsymbol{x}} \dfrac{\partial \boldsymbol{\varphi}_i}{\partial t}} \frac{\partial q_{i+1}}{\partial \theta_{i+1}} \frac{\partial \boldsymbol{\varphi}_i}{\partial t} \right] \frac{\partial \boldsymbol{\varphi}_i}{\partial \boldsymbol{x}_i}, \tag{9}$$

$$\frac{\partial T}{\partial \boldsymbol{y}_0} = \frac{\partial \eta}{\partial \boldsymbol{x}} \left(\prod_{i=1}^{m} \frac{\partial T_{m-i}}{\partial \boldsymbol{x}_{m-i}} \right) \frac{\partial \eta^{-1}}{\partial \boldsymbol{y}}, \tag{10}$$

$$\frac{\partial T_{j-1}}{\partial \theta_j} = \frac{-1}{\dfrac{\partial q_j}{\partial \boldsymbol{x}} \dfrac{\partial \boldsymbol{\varphi}_{j-1}}{\partial t}} \frac{\partial q_j}{\partial \theta_j} \frac{\partial \boldsymbol{\varphi}_{j-1}}{\partial t}, \tag{11}$$

$$\frac{\partial T}{\partial \theta_j} = \frac{\partial \eta}{\partial \boldsymbol{x}} \prod_{i=1}^{m-j} \frac{\partial T_{m-i}}{\partial \boldsymbol{x}_{m-i}} \frac{\partial T_{j-1}}{\partial \theta_j}. \tag{12}$$

We can suppose here that $(\partial q_{i+1}/\partial \boldsymbol{x}) \times (\partial \boldsymbol{\varphi}_i/\partial t)$ and $(\partial q_j/\partial \boldsymbol{x}) \times (\partial \boldsymbol{\varphi}_{j-1}/\partial t)$ are non-zero values unless the orbit and sections are crossed tangentially.

Suppose that $\boldsymbol{\xi}(k)$ is a small perturbation and $u(k)$ is intended to be a control input defined later. When the parameter θ_j is chosen as a controlling parameter, the variational equations around the fixed point are expressed as

$$\boldsymbol{y}(k) = \boldsymbol{y}^* + \boldsymbol{\xi}(k),\ \theta_j(k) = \theta_j + u(k). \tag{13}$$

After one iteration of T, we have

$$\begin{aligned} \boldsymbol{y}(k+1) &= T(\boldsymbol{y}^* + \boldsymbol{\xi}(k),\ \theta_j + u(k)) \\ &\approx \boldsymbol{y}^* + \frac{\partial T}{\partial \boldsymbol{y}^*} \boldsymbol{\xi}(k) + \frac{\partial T}{\partial \theta_j} u(k). \end{aligned} \tag{14}$$

Therefore we obtain the difference equation defined by the derivative of T as follows:

$$\boldsymbol{\xi}(k+1) = D_{\boldsymbol{y}^*} \boldsymbol{\xi}(k) + D_{\theta_j} u(k), \tag{15}$$

where $D_{\boldsymbol{y}^*} = \partial T/\partial \boldsymbol{y}^*$ and $D_{\theta_j} = \partial T/\partial \theta_j$. Note that Eq. (15) holds when the state $\boldsymbol{y}(k)$ is located to be adjacent to the fixed point $\boldsymbol{y}^*$.

To stabilize $\boldsymbol{\xi}(k)$ at the origin, a state feedback control is designed as follows [Ueta & Kawakami, 1995]:

$$u(k) = C^\top \boldsymbol{\xi}(k), \tag{16}$$

where $\top$ is a transpose and C is an appropriate $n-1$ dimensional vector designed by the pole assignment method. Thus we have

$$\boldsymbol{\xi}(k+1) = [D_{\boldsymbol{y}^*} + D_{\theta_j} C^\top] \boldsymbol{\xi}(k). \tag{17}$$

The corresponding characteristic equation is given by

$$\chi(\mu) = \det(D_{\boldsymbol{y}^*} + D_{\theta_j} C^\top - \mu I) = 0. \tag{18}$$

The stability condition at the origin is $|\mu_i| < 1,\ i = 1,\ 2,\ \ldots,\ n-1$.

In the conventional chaos control methods, a control input is applied into the specific system parameter as a small perturbation. During a transition state, the control system consumes a certain control energy given by integration of such perturbations. Thus $\epsilon = \int_0^\infty ||u(t)|| dt$ is regarded as the controlling energy. In our method, the control input $u(k)$ is added into θ_j; see Eq. (13). Figure 1 depicts a schematic diagram of the method. The location of the section Π_0 defined by θ_0 is shifted by $u(k)$ instantly when the orbit $\boldsymbol{\varphi}_0(t,\ \boldsymbol{x}_0)$ departs from Π_0. No actual control input is added into the system. The state-feedback is utilized only to determine the dynamic threshold value, thus the orbit starting from the current threshold value reaches the next controlled threshold value without any control energy.

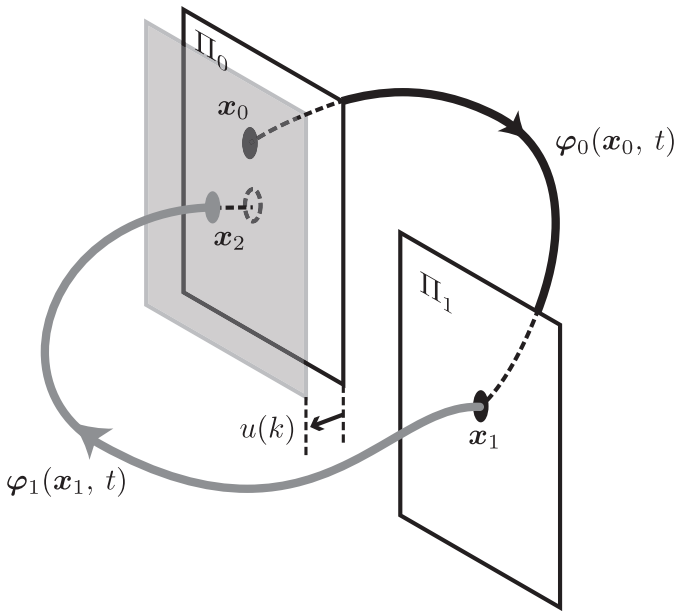

Fig. 1. Relationship between the flow and sections. Our method adjusts the position of the local section Π_0 only. The state and vector fields are not affected by the control input.

3. A simple chaotic system

Let us consider a simple interrupt chaotic system [Kousaka *et al.*, 2001] shown in Fig. 2 as an example. The switch is flipped by a certain rule depending on the state and the period. Assume that v is the state

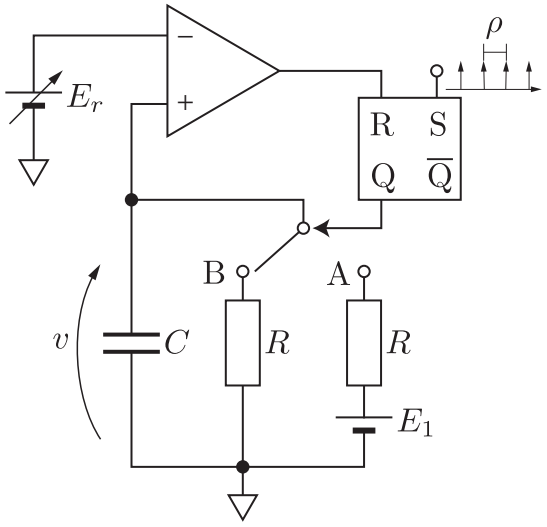

Fig. 2. Circuit model of interrupt chaotic system. ρ and E_r represent the period of the clock pulse input and the switching threshold value, respectively.

variable, and then the normalized equation is given as follows:

$$\begin{gathered} \dot{v} = -v + E, \\ \text{if} \quad t = n \cdot \rho \quad \text{then} \quad E \leftarrow E_1, \quad \text{if} \quad v > E_r \quad \text{then} \quad E \leftarrow 0, n \in \mathbb{N}^0, \end{gathered} \tag{19}$$

where E_1 and E_r are a direct current bias and a switching threshold value, respectively. ρ is the period of the clock pulse input. Figure 3 illustrates the behavior of the dynamics. If the Poincaré section is defined as $\Pi = \{v \in \boldsymbol{R};\ t = n\rho\}$, trajectories stroke two types of solutions (Fig. 4), and they can be solved exactly,

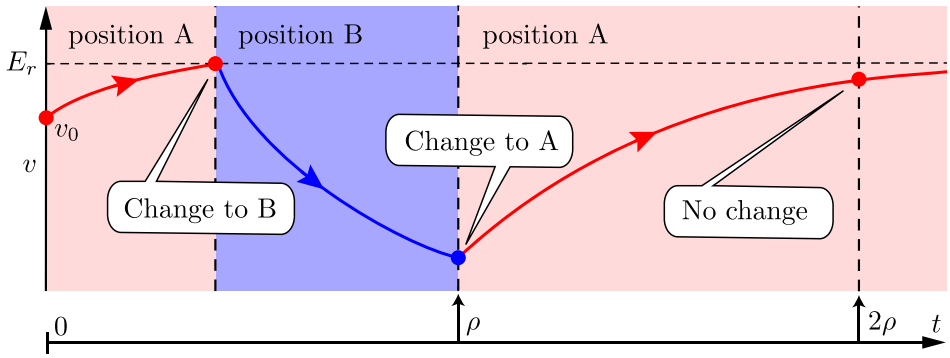

Fig. 3. The switching behavior. When the capacitor voltage reaches to the threshold value E_r, the switch is flipped to the position B. If the time t is ρ, the switch is flipped to the position A.

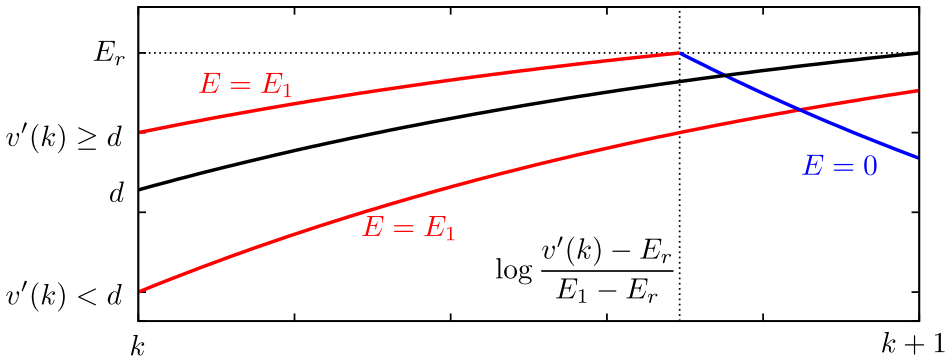

Fig. 4. The sketch of a simple chaotic interrupt system. There are two types of trajectories depending on the initial value $v'(k)$. If $v'(k)$ is less than d, the trajectory reaches $v'(k+1)$ without interruption. Otherwise, the trajectory reaches the threshold value E_r, and E is changed to zero.

see, [Kousaka *et al.*, 2000]. Therefore the system can be discretized by the Poincaré section, and redefined as follows:

$$v'(k+1) = g(v'(k)) = \begin{cases} (v'(k) - E_1)e^{-\rho} + E_1, & (v'(k) < d), \\ E_r \dfrac{v'(k) - E_1}{E_r - E_1} e^{-\rho}, & (v'(k) \geq d), \end{cases} \tag{20}$$

$$d = (E_r - E_1)e^{\rho} + E_1. \tag{21}$$

Note that $v'(k) = v(k\rho)$. The solution ψ is defined by Eq. (22):

$$\psi(v'(0), k) = v'(k), \ \psi(v'(0), 0) = v'(0) = v(0). \tag{22}$$

A chaotic attractor and three UPOs with parameters $E_1 = 3$, $E_r = 2.5$ and $\rho = 0.606$ are shown in Fig. 5. Table 1 lists the periods, states and multipliers of each UPO. Each orbit is confirmed to be a UPO.

From Eqs. (17) and (18), the control gain is given as follows:

$$C = \frac{q - D_{v^*}}{D_{E_r}}, \tag{23}$$

where $D_{v^*} = \partial T / \partial v^*$ and $D_{E_r} = \partial T / \partial E_r$ are derivatives of T, and can be calculated by Eqs. (24) and (25).

$$\frac{\partial T}{\partial v^*} = \frac{\partial \psi}{\partial v^*}(v^*, \ p), \ \frac{\partial \psi}{\partial v^*}(v^*, \ k+1) = \left.\frac{\partial g}{\partial v'}\right|_{v'=v'(i)} \frac{\partial \psi}{\partial v^*}(v^*, \ k), \ \frac{\partial \psi}{\partial v^*}(v^*, \ 0) = I, \tag{24}$$

$$\frac{\partial T}{\partial E_r} = \frac{\partial \psi}{\partial E_r}(v^*, \ p), \ \frac{\partial \psi}{\partial E_r}(v^*, \ k+1) = \left.\frac{\partial g}{\partial v'}\right|_{v'=v'(i)} \frac{\partial \psi}{\partial v^*}(v^*, \ k) + \left.\frac{\partial g}{\partial E_r}\right|_{v'=v'(i)}, \ \frac{\partial \psi}{\partial E_r}(v^*, \ 0) = 0, \tag{25}$$

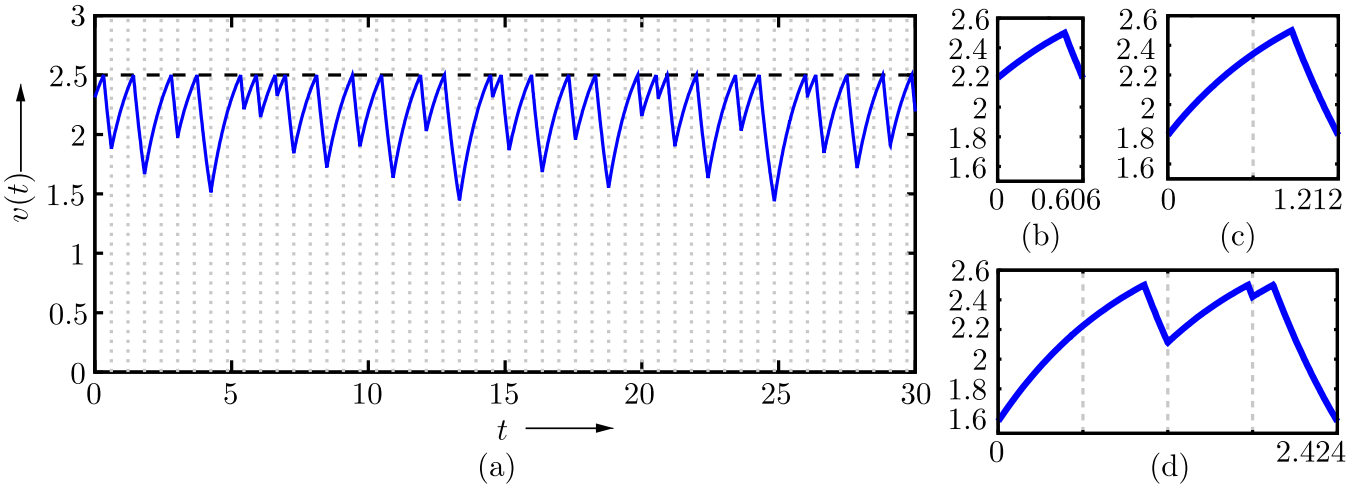

Fig. 5. Trajectories of a chaotic attractor and UPOs embedded into the chaos.

Table 1. Periods, states and multipliers of UPOs in Fig. 5.

attractor	period	v^*	μ
(b) UPO_1	1	2.195202	−2.727643125796
(c) UPO_2	2	1.794216	−1.488007404341
		2.34221	
(d) UPO_4	4	1.580281	−11.070830176867
		2.225503	
		2.112552	
		2.420642	

where the symbol $p \in \mathbb{N}^+$ is the period of the target trajectory, and q is a desirable pole for the controlling, and $|q| < 1$ is required for stabilization. When the clock pulse is input at $t = k\rho$, $u(t)$ is generated as $C(v^* - v'(k))$ from Eq. (16), and it is added to the switching threshold E_r. Figure 6 shows the behavior of $u(t)$ and the system. When $u(t)$ is applied to the system, the threshold value is changed, and the behavior of the system is controlled.

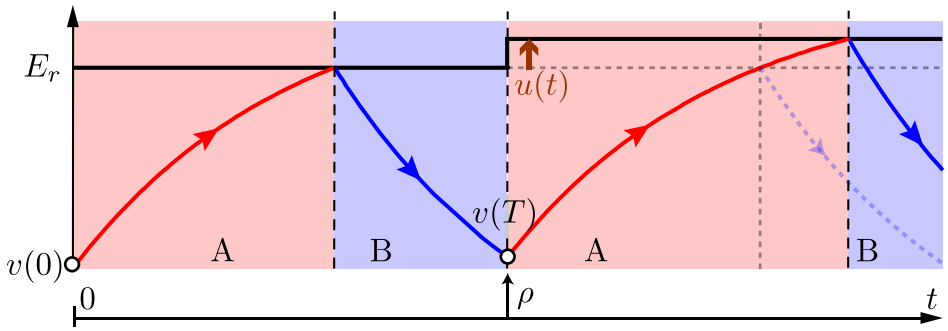

Fig. 6. Controller affects the switching threshold E_r, thus the control input $u(t)$ biases E_r. By doing this, the controller can control the trajectory without any effect on the dynamical equations and vector fields.

3.1. *Numerical simulation*

We show some results of the chaos control by referring to Fig. 7, where each graph shows a transition response of the orbit and the threshold value. From this figure, we confirm that each UPO is controlled to

achieve a stable periodic orbit by several renewals of $u(t)$. The UPO_4 in Fig. 7 (c) has a longer renewal span than other UPOs because a renewal span depends on the period of the target UPO.

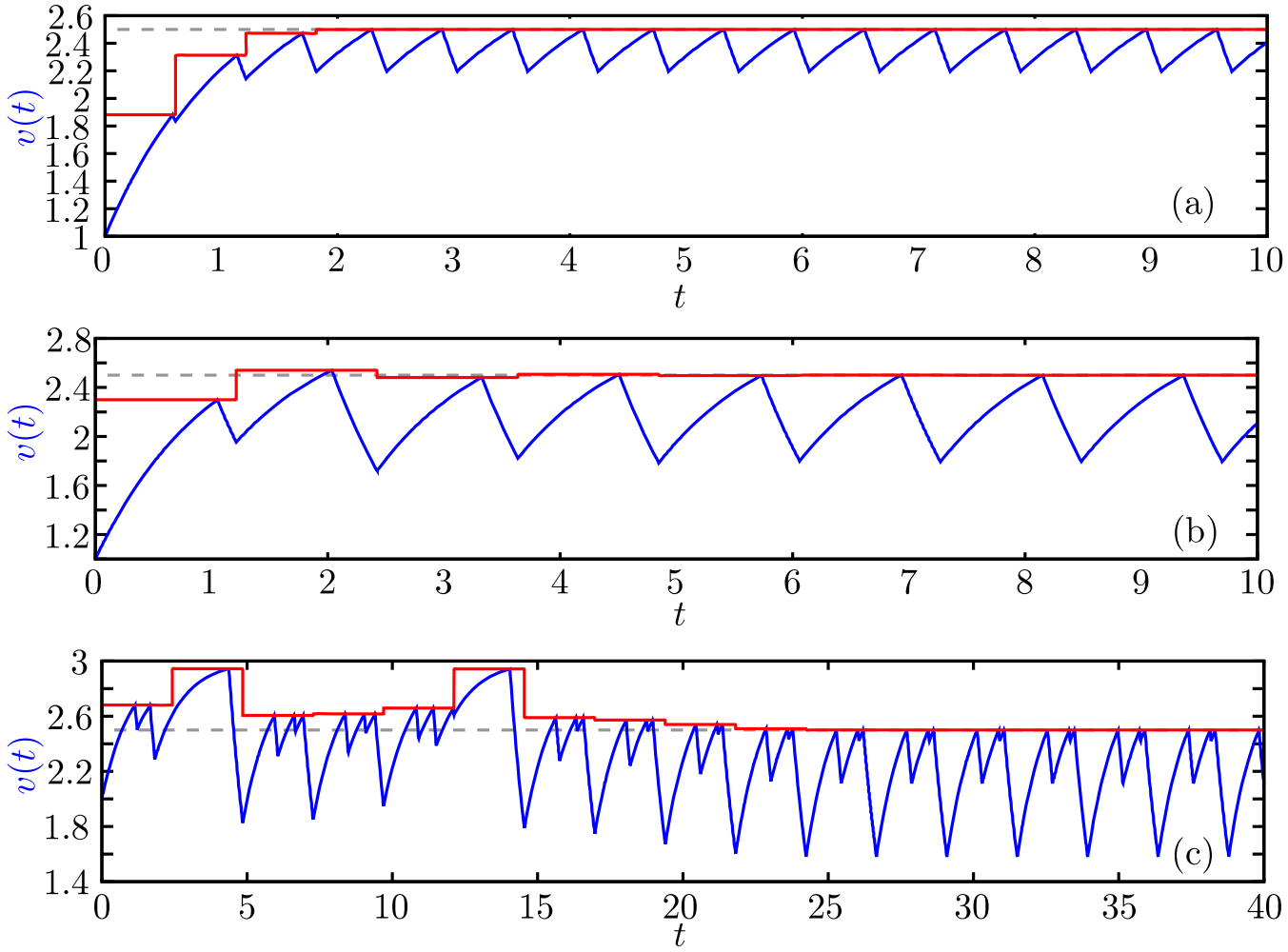

Fig. 7. Transition responses of controlled UPOs and the threshold values. (a) Period-1, (b) period-2 and (c) period-4 solutions shown in Tab. 1 are stabilized. Note that $u(t)$ does not affect the state and vector fields directly.

Figure 8 shows basins of attraction of UPOs with our controller in the q-$v(0)$ plane. White pixels in the figure indicate the initial values in which the UPO could be stabilized, and black pixels indicate failure of the controlling. This shows that all UPOs could be stabilized easily with relatively small initial values. Additionally, UPOs can also be stabilized at a negative initial value. However, in larger initial values, the UPO_4 could not be controlled. The pole assignment method renews the control signal on a periodic basis only. Therefore, this technique is less effective for long-period UPOs such as the UPO_4.

Figure 5 (a) reveals that the chaotic attractor wanders within $1.3 < v(t) < 2.5$. The basin of attraction in this range is shown by white pixels in Fig. 8. Thus the UPO_1 and the UPO_2 are stabilized robustly. The threshold control performs well for this simple chaotic system.

3.2. *Circuit implementation*

Owing to the sample holder synchronized with a clock pulse, our controller is very easy to implement, thus we show the circuit implementation and experimental results.

Figure 9 shows the circuit diagram of the system and the controller. The subtractor and the inverter 1 generate $u(t)$, and the adder and the inverter 2 add the control input to the switching threshold. The

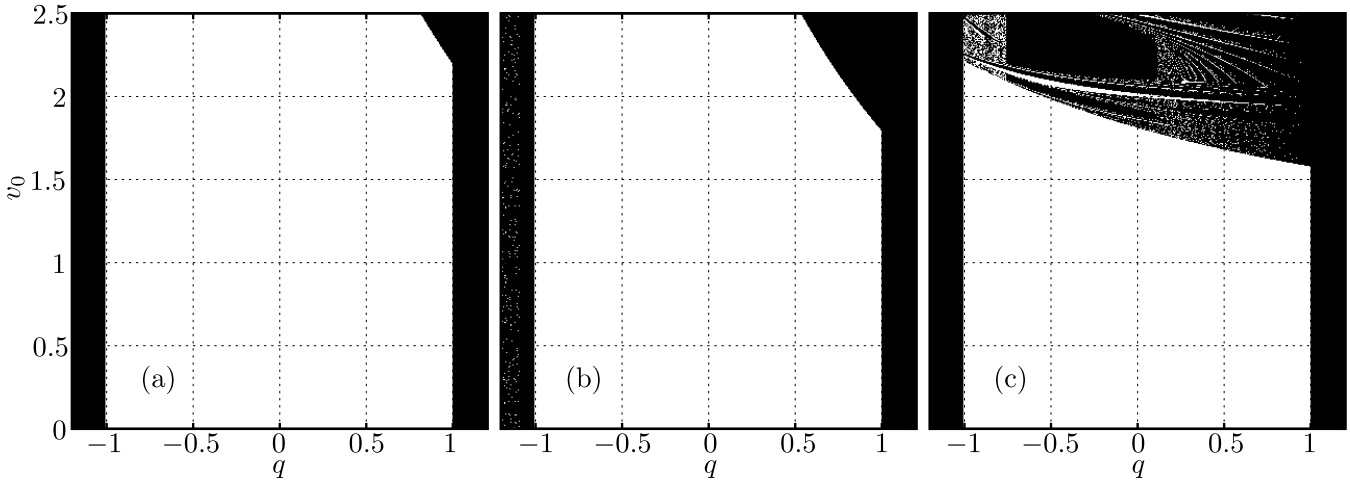

Fig. 8. Basins of attraction resulting from a control experiment. (White: stabilizable regions and black: unstabilizable regions.) The horizontal and vertical axes are the parameter q of the controller and the initial state of the system, respectively.

switching threshold generated by this controller is applied to the system as a perturbation of the reference value E_r. We use ICs TC4053BP and LM325M as the logic switch and the comparator in this experiment.

Figure 10 shows a transition response of the circuit experiment. In these figures, the top, 2nd, 3rd and bottom time series show the clock pulse input, the timing of the renewal of the control signal, the voltage of the capacitor as the orbit v and the control signal, respectively. It is confirmed that control inputs converged to zero, and orbits are certainly stabilized at UPOs.

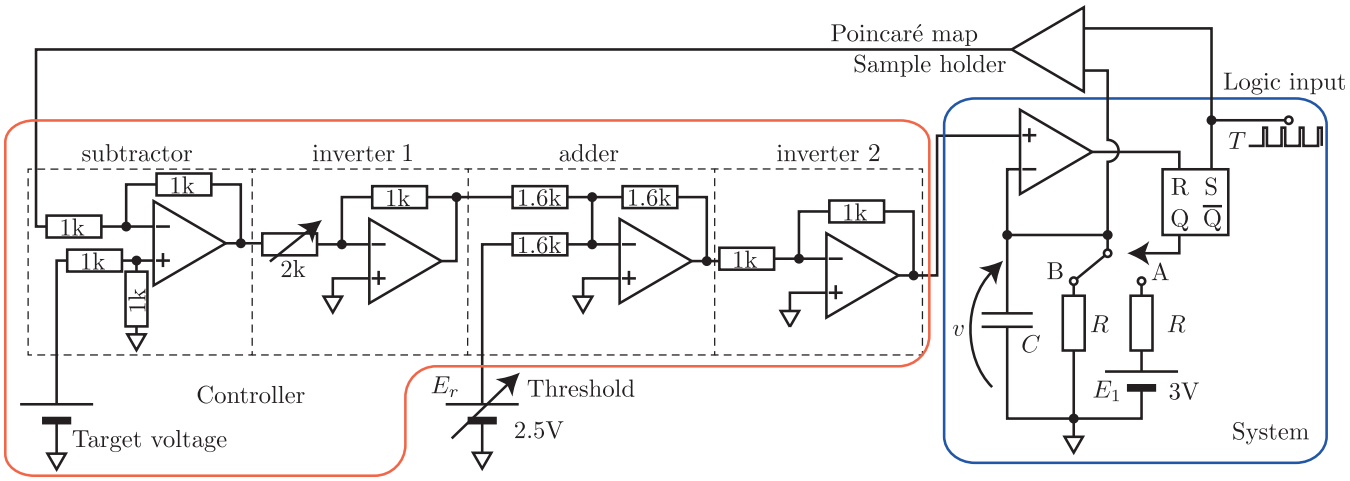

Fig. 9. Circuit diagram of a simple chaotic system and the proposed controller. The controller is composed of four parts. The variable resistance defines the controlling gain, and the voltage source is the target voltage v^*.

4. Izhikevich model

Let us consider the Izhikevich model [Izhikevich, 2003] as the second example. As is well known that this model is two dimensional, and behaves chaotically in certain parameter setting [Tamura *et al.*, 2009]. The equations are given as follows:

$$\dot{\boldsymbol{v}}(t) = \begin{pmatrix} 0.04v + 5v + 140 - w + I \\ a(bv - w) \end{pmatrix}, \tag{26}$$

$$\text{if} \quad v = \theta, \quad \text{then} \quad v \leftarrow c, \quad w \leftarrow w + d, \tag{27}$$

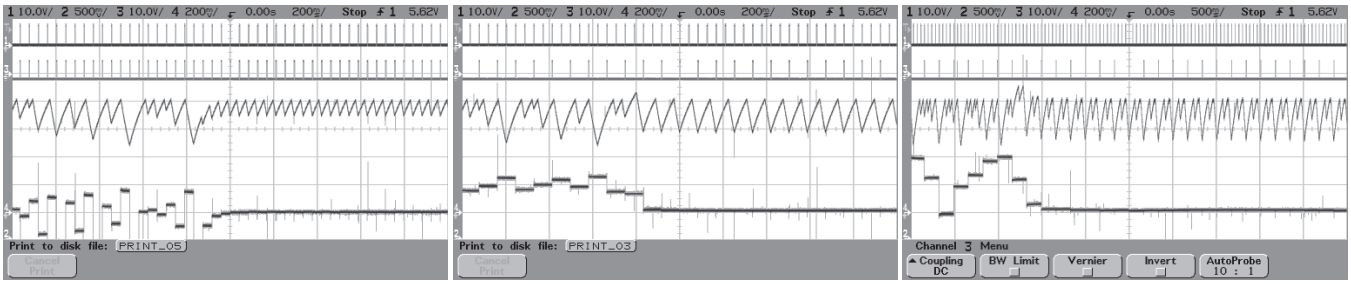

Fig. 10. Results of stabilizing the UPO_1, UPO_2, and UPO_4 are (a), (b) and (c), respectively. (Top: the clock pulse input, 2nd: the timing of the renewal of the controlling signal, 3rd: the voltage of the capacitor [10V/DIV], and bottom: the control input voltage [200mV/DIV]. The horizontal axis: time [(a, b) 200 and (c) 500msec/DIV].) The controlling started about 800 msec. The circuit is quickly converged to each periodic orbit after start-up of the control.

where $\boldsymbol{v} = (v,\ w)$ is the state, and I, a, b, c, d and θ are parameters. Especially, c and d show the jumping dynamics, and θ defines the threshold value of the jumping. Figure 11 illustrates the behavior of the dynamics.

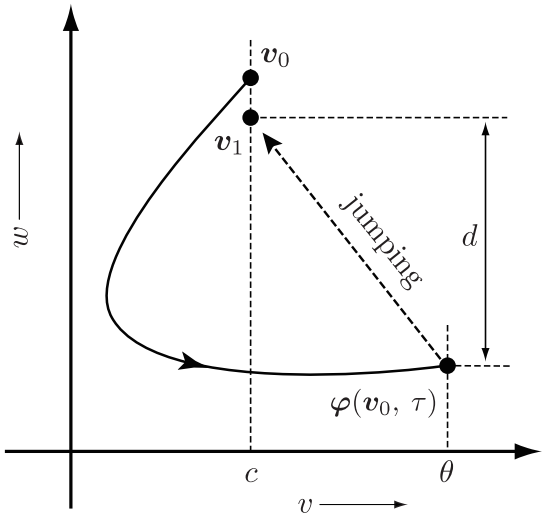

Fig. 11. The sketch of the typical behavior of the Izhikevich model. If the state $\boldsymbol{v}(t)$ reaches the threshold value θ, the state $\boldsymbol{v}(t) = (\theta,\ w(t))$ jumps to $\boldsymbol{v}(t) = (c,\ w(t) + d)$.

A chaotic attractor and three UPOs that are involved in it with parameters $a = 0.2$, $b = 2$, $c = -56$, $d = -16$, $I = -99$ and $\theta = 30$ are shown in Fig. 12. Table 2 lists the periods, states and multipliers of several UPOs. Each orbit is confirmed to be a UPO.

Table 2. Periods, states and multipliers of UPOs in Fig. 12.

attractor	period	w^* $(v^* = c = 56)$	μ
UPO_1	1	−111.734371227672	−2.192843924301
UPO_2	2	−114.280257572631	−9.910331534347
		−109.950121533113	
UPO_3	3	−114.603487249294	+25.322864600880
		−112.427919143969	
		−109.602553091223	

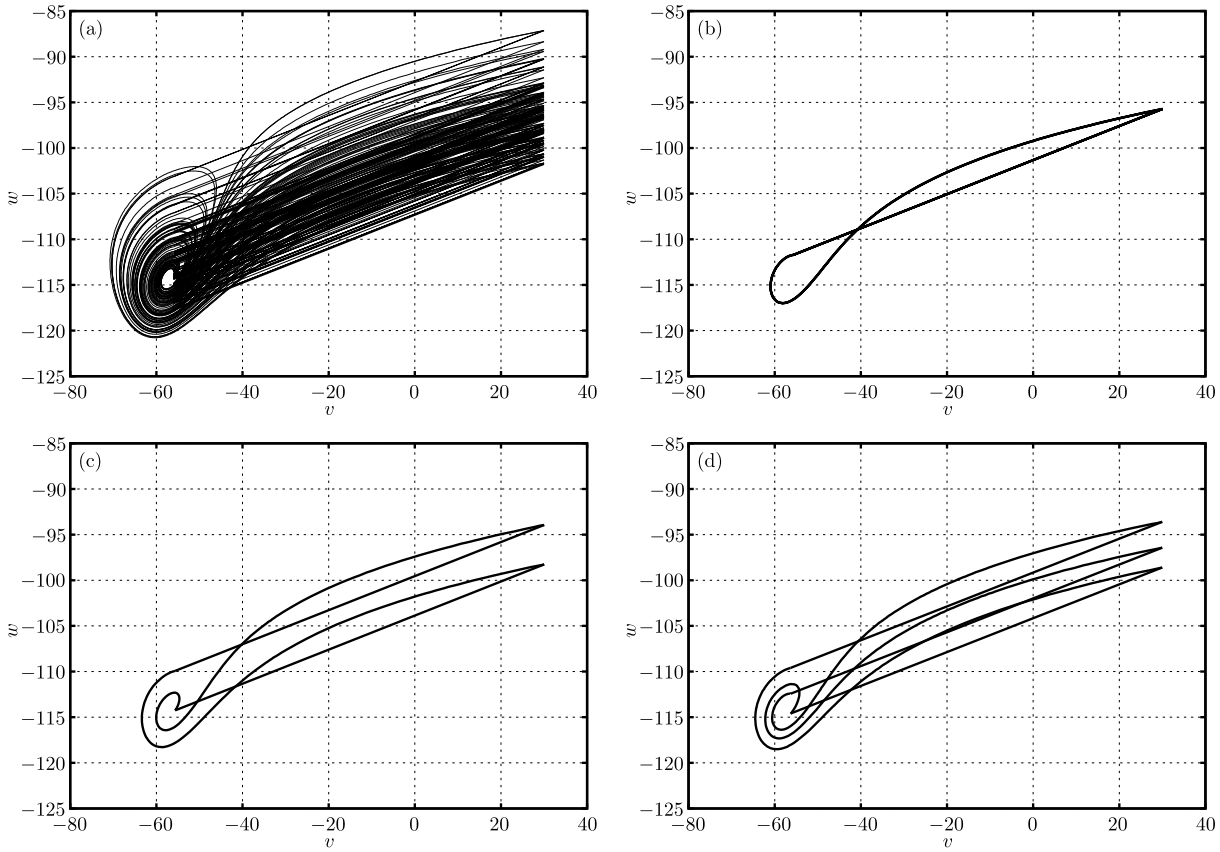

Fig. 12. Phase portraits of a chaotic attractor and UPOs by the numerical simulation, where $a = 0.2$, $b = 2$, $c = -56$, $d = -16$ $I = -99$ and $\theta = 30$. These UPOs are embedded in the chaotic attractor.

4.1. *Controller*

The stabilizing control is applied to UPOs in Table 2. The Poincaré section is defined as: $\Pi = \left\{ \boldsymbol{x} \in \boldsymbol{R}^2 |\ q(\boldsymbol{x}) = v - \theta = 0 \right\}$.

From Eqs. (17) and (18), the control gain is computed as follows:

$$C = \frac{q - D_{w^*}}{D_\theta}, \tag{28}$$

where $D_{w^*} = \partial T / \partial w^*$ and $D_\theta = \partial T / \partial \theta$. The derivative of the Poincaré map by the threshold value θ are obtained by Eqs. (9)–(12). Now q is a desirable pole for the controller, and $|q| < 1$ is required for stabilization. The control input $u(k)$ is generated by the gain $C \in \boldsymbol{R}$ and the state $\boldsymbol{v}(t)$ as $C(w^* - w(\tau))$ from Eq. (16). It is renewed after the jumping dynamics, and added to the threshold value θ as a perturbation. Since θ is only referred as the threshold value of the jumping dynamics, $u(k)$ does not affect the dynamical equations during the transition state.

4.2. *Numerical simulation*

We show some results of the chaos control in Fig. 13, where each diagram shows a transition response of the orbit and the threshold value with the controlling signal. From these figures, we confirmed that each UPO has been controlled to achieve a stable periodic orbit by several renewals of $u(t)$. To prevent generating big amplitude of the control, a limiter is provided in the controller. The condition is given as follows:

$$\text{if} \quad |u(t)| \geq 20 \quad \text{then} \quad u(t) \leftarrow 0. \tag{29}$$

Figure 14 shows the basins of attraction of UPOs with our controller in the q-$w(0)$ plane. White pixels in Fig. 14 indicate the initial values in which the UPO can be stabilized, and black pixels indicate failure of the controlling.

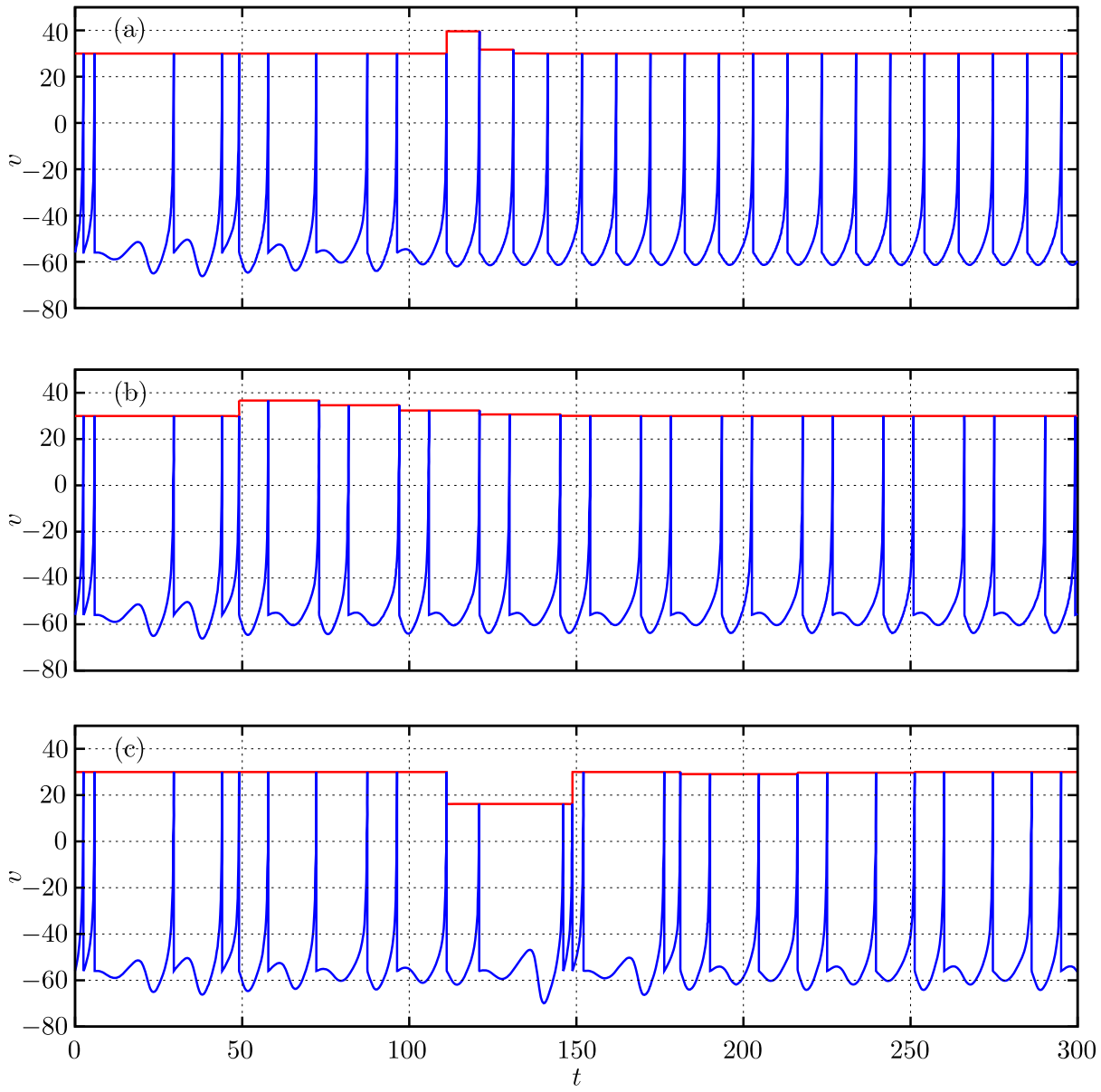

Fig. 13. Transition responses of controlled UPOs and the threshold values. (a) Period-1, (b) period-2 and (c) period-3 solutions shown in Table 2 are stabilized, and the final threshold value is 30[mV]. Note that $u(t)$ is not applied to the system as a continuous input, but only updates the threshold value.

Figure 12 reveals that the chaotic attractor wanders within $-125 < w < -100$ on the Poincaré section. The basin of attraction in this range is shown by the white regions in Fig. 14. Thus UPOs are stabilized robustly, and the threshold control for the piecewise nonlinear system performs well.

5. Conclusion

We have proposed a control method for UPOs embedded in hybrid chaotic systems by variable threshold values. First, we have explained how to design the controlling gain of assigning poles with the perturbation of a switching threshold. The pole assignment method requires the derivatives of the Poincaré map about threshold values, for which we have proposed the technique to calculate. We have also demonstrated the design of a controller and numerical simulations of the controlling for a 1D switching chaotic system and a 2D chaotic neuron model. Some simulation results indicate that our controller stabilizes object UPOs well. Additionally, we have implemented our controller in a real circuit and presented experimental results.

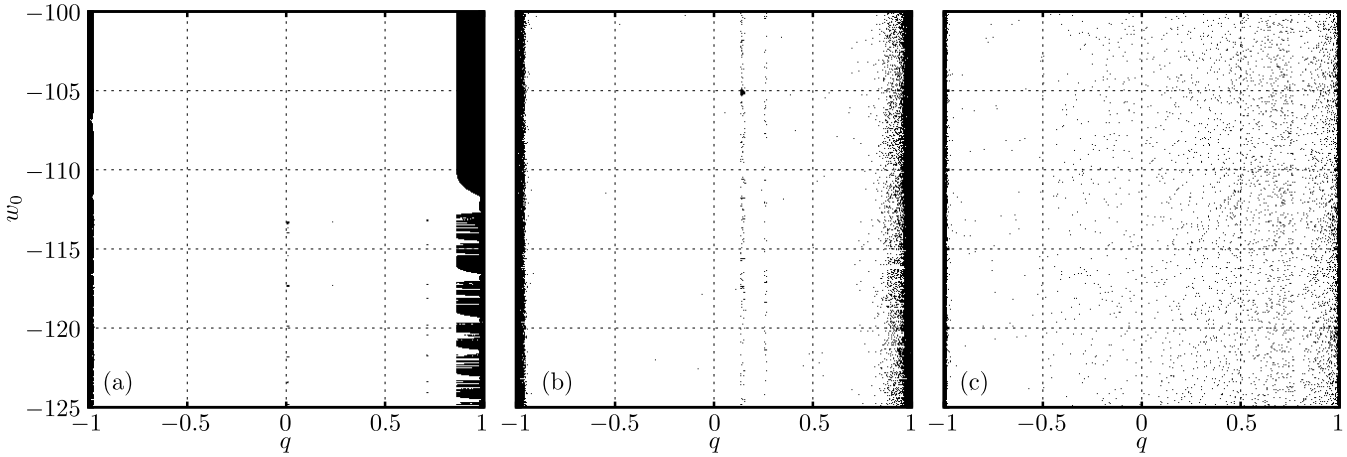

Fig. 14. Basins of attraction resulting from a control experiment. (White: stabilizable regions and black: unstabilizable regions.) The horizontal and vertical axes are the parameter q of the controller and the initial state of the system, respectively.

From them, it is confirmed that our controller can be implemented in a real circuit, and also well performed without technical difficulties.

For modeling biological and medical systems, the hybrid dynamical systems are widely used [Aihara & Suzuki, 2010]. For example, Akakura *et al.* [Akakura *et al.*, 1993] reported that the intermittent hormone therapy can be effective in the treatment of prostate cancer. This therapy switches the treatment of hormone therapy on and off based on the observation of the serum prostate-specific antigen (PSA) level. Therefore, the therapy can be represented as a hybrid dynamical system, and some PSA levels are defined as the switching threshold values. The mathematical modeling of the intermittent hormone therapy has been investigated intensively [Tanaka *et al.*, 2010; Hirata *et al.*, 2010]. Since our method is available for general piecewise nonlinear systems and the threshold perturbation seems to be related to the intermittent hormone therapy, it is worth investigating a possibility whether our method is applicable for the prostate cancer treatment or not.

Acknowledgments

This research is partially supported by the Aihara Project, the FIRST program from the Japan Society for the Promotion of Science (JSPS), initiated by the Council for Science and Technology Policy (CSTP), and by JSPS KAKENHI Grant Number 25420373.

References

Aihara, K. & Suzuki, H. [2010] "Theory of hybrid dynamical systems and its applications to biological and medical systems," *Phil. Trans. R. Soc. A. 13* **368**, 4893–4914.

Akakura, K., Bruchovsky, N., Goldenberg, S. L., Rennie, P. S., Buckley, A. R. & Sullivan, L. D. [1993] "Effects of intermittent androgen suppression on androgen-dependent tumors. Apoptosis and serum prostate-specific antigen," *Cancer* **71**, 2782–279.

Auerbach, D., Cvitanović, P., Eckmann, J.-P. & Gunaratne, G. [1987] "Exploring chaotic motion through periodic orbits," *Phys. Rev. Lett.* , 2387–2389.

Bernardo, M., Budd, C. J., Champneys, A. R. & Kowalczyk, P. [2008] *Piecewise-smooth Dynamical Systems: Theory and applications* (London, U. K.: Springer-Verlag, London).

Hirata, Y., Bruchovsky, N. & Aihara, K. [2010] "Development of a mathematical model that predicts the outcome of hormone therapy for prostate cancer," *Journal of Theoretical Biology* **264**, 517–527.

Inagaki, T. & Saito, T. [2008] "Consistency in a chaotic spiking oscillator," *IEICE Trans. Fundamentals* **E91-A**, 2040–2043.

Ito, D., Ueta, T. & Aihara, K. [2010] "Bifurcation analysis of two coupled Izhikevich oscillators," *Proc. NOLTA2010* (Poland), pp. 627–630.

Izhikevich, E. M. [2003] "Simple model of spiking neurons," *IEEE Trans. Neural Networks* **14**, 1569–1572.
Kousaka, T., Kido, T., Ueta, T., Kawakami, H. & Abe, M. [2000] "Analysis of border-collision bifurcation in a simple circuit," *Proc. ISCAS 2000* (Geneva), pp. 481–484.
Kousaka, T., Tahara, S., Ueta, T., Abe, M. & Kawakami, H. [2001] "Chaos in simple hybrid system and its control," *Electronics Letters* **37**, 1–2.
Kousaka, T., Ueta, T. & Kawakami, H. [1999] "Bifurcation of switched nonlinear dynamical systems," *IEEE Trans. Circuits and Syst.* **CAS-46**, 878–885.
Kousaka, T., Ueta, T. & Kawakami, H. [2002] "Controlling chaos in a state-dependent nonlinear system," *International Journal of Bifurcation and Chaos* **12**, 1111–1119.
Kousaka, T., Ueta, T., Ma, Y. & Kawakami, H. [2006] "Control of chaos in a piecewise smooth nonlinear system," *Chaos, Solitons & Fractals* **27**, 1019–1025.
Leine, R. & Nijmeijer, H. [2004] *Dynamics and Bifurcations of Non-smooth Mechanical Systems* (Berlin: Springer-Verlag, Berlin).
Murali, K. & Sinha, S. [2003] "Experimental realization of chaos control by thresholding," *Phys. Rev. E* **68**, 016210.
Myneni, K., Barr, T. A., Corron, N. J. & Pethel, S. D. [1999] "New method for the control of fast chaotic oscillations," *Phys. Rev. Lett.* **83**, 2175–2178.
Ott, E., Grebogi, C. & Yorke, J. A. [1990] "Controlling chaos," *Phys. Rev. Lett.* **64**, 1196–1999.
Perc, M. & Marhl, M. [2004] "Detecting and controlling unstable periodic orbits that are not part of a chaotic attractor," *Phys. Rev. E* **70**, 016204.
Perc, M. & Marhl, M. [2006] "Chaos in temporarily destabilized regular systems with the slow passage effect," *Chaos, Solitons & Fractals* **27**, 395–403.
Pyragas, K. [1992] "Continuous control of chaos by self-controlling feedback," *Phys. Lett. A* **170**, 421–428.
Pyragas, K. [2006] "Delayed feedback control of chaos," *Phil. Trans. R. Soc. A 15* **364**, 2309–2334.
Rajasekar, S. [1993] "Controlling of chaos by weak periodic perturbations in Duffing-van der Pol oscillator," *Pramana* **41**, 295–309.
Rajasekar, S. & Lakshmanan, M. [1993] "Algorithms for controlling chaotic motion: application for the BVP oscillator," *Physica D* **67**, 282–300.
Romeiras, F. J., Grebogi, C., Ott, E. & Dayawansa, W. P. [1992] "Controlling chaotic dynamical systems," *Physica D* **58**, 165–192.
Roy, R., Murphy, T. W., Maier, T. D., Gills, Z. & Hunt, E. R. [1992] "Dynamical control of a chaotic laser: Experimental stabilization of a globally coupled system," *Phys. Rev. Lett.* **68**, 1259–1262.
Sabuco, J., Zambrano, S. & Sanjuán, M. A. F. [2010] "Partial control of chaotic transients using escape times," *New J. Phys.* **12**, 113038.
Starrett, J. [2003] "Control of chaos by occasional bang-bang," *Phys. Rev. E* **67**, 036203.
Tamura, A., Ueta, T. & Tsuji, S. [2009] "Bifurcation analysis of izhikevich neuron model," *Dynamics of Continuous, Discrete and Impulsive Systems* **16**, 849–862.
Tanaka, G., Hirata, Y., Goldenberg, S. L., Bruchovsky, N. & Aihara, K. [2010] "Mathematical modelling of prostate cancer growth and its application to hormone therapy," *Phil. Trans. R. Soc. A. 13* **368**, 5029–5044.
Ueta, T. & Kawakami, H. [1995] "Composite dynamical system for controlling chaos," *IEICE Trans. Fundamentals* **E78-A**, 708–714.
Zambrano, S. & Sanjuán, M. A. F. [2009] "Exploring partial control of chaotic systems," *Phys. Rev. E* **79**, 026217.